Diagrams finished volumes SUSHI for the modelization of miscible unsaturated flows

Summarized:

This note briefly presents the diagrams finished volumes developed in Code_Aster. A short recall of the equations of behavior concerned is carried out then the diagrams used are presented.

Contents

1 Introduction3
2 Presentation of problem: Assumptions, Notations3
2.1 Tallies of modélisation3
2.2 Notations3
2.2.1.1 Variables of état4
2.2.1.2 Quantities characteristic of the phase solide4
2.2.1.3 Quantities characteristic of the fluides4
2.3 Constitutive equations of the modèle5
2.3.1 Equations of équilibre5
2.3.2 Equations of comportement5
2.3.2.1 Constitutive laws of the fluides5
2.3.2.2 Equations of diffusion6
the 3 diagrams finished volumes implemented in Code_Aster6
3.1 General information on finis7 volumes
3.2 finished volumes SUSHI applied to diphasic flows miscibles7
3.2.1 Choices of the inconnues8
3.2.2 Choices of volume of contrôle8
3.2.3 Writing of the flux8
3.2.4 Décentrage10
4 Implementation in Code_Aster16
4.1 Description of elements 16.4.2
Computation of the stresses and strains généralisées17
4.3 Intégration19
4.4 Variables internes20
4.5 Validation20
5 Bibliographie21
6 Description of the versions of document21

1 Introduction

We present here the diagrams finished volumes SUSHI developed for the modelization of diphasic flows (unsaturated) miscible in porous environment, miscible meaning here that the components can exist under several phases. These diagrams concern the family of modelizations THM. They are planned only for the pure hydraulics (neither mechanics, nor thermal), that is to say if one takes again the classical nomenclature described in [R7.01.11] `the KIT_HH`.

The diagrams finished volumes SUSHI (Design Using Stabilization and Hybrid Interfaces) were developed by Ophélie Angelini in the frame of its thesis 21 in particular to deal with stiff problems of fronts on unspecified meshes. This diagram is inspired by the diagram Hybid Finite Volume (HVF) introduced by R. Eymard and al.21. At the origin of this work, an abundant literature was indicating that these diagrams ensuring by definition a good representation of flux were adapted to this kind of hyperbolic equations applied to strongly heterogeneous fields. To establish and have such diagrams thus quickly appeared reasonable would be to only compare itself with the members of the community of flows in porous environment 21. These diagrams do not claim to replace the finite elements but propose a robust alternative.

We will present here only briefly the model physical diphasic flows detailed in documentation [R7.01.11].

This documentation thus presents primarily the diagrams of spatial discretization Finished Volumes implemented on these models in Code_Aster. For further details, one will refer to the thesis of Ophélie Angélini 21

2 Presentation of problem: Assumptions, Notations

the group of the hydraulic physical model is presented in detail in R7.01.11. One is satisfied here to point out the principal variables and assumptions as well as the treated equations. The formalism is primarily resulting from works of Coussy 21. The routines managing the constitutive laws are not impacted by the use of the diagram finished volume.

2.1 Tally of modelization

These developments relate to only the models with 2 phases (liquidates gas) and 2 miscible components (for example water and hydrogen). We thus place ourselves in the frame as of modelizations *_HH2 (cf U2.04.05). More precisely one will speak here about modelizations `HH2SUC`, `HH2SUDA`, `HH2SUDM` (cf section 16).

It is pointed out that the 2 hydraulic constitutive laws that one can use are then:

- `LIQU_AD_GAZ_VAPE` : 2 components per phase
- `LIQU_AD_GAZ` : 2 components in the liquid phase, only one in the phase gas (neglected vapor)

In the continuation one will not speak that complete model with 2 components, 2 phases. The case without vapor amounts right cancelling the terms relating to it.

2.2 Notations

We suppose that the pores of solid are occupied by two components noted w (for water) and h (for hydrogen), each one coexistent in two phases to the maximum, one liquidates noted l and the other gas one noted g.
The quantities A associated with the phase p ($p=l,g$) with the component c will be noted: X_p^c.
Concretely, that gives:

- A_l^w : quantity A for liquid water

- A_g^w : quantity A for the steam
- A_l^h : quantity A for the component H dissolved in the fluid
- A_g^h : quantity A for the component H in gas form (e.g. dry hydrogen).

The general assumptions carried out are the following ones:

- anisotropic behavior,
- the gases are perfect gases,
- mixes ideal perfect gases (stagnation pressure = sum of the partial pressures),
- thermodynamic equilibrium between the phases of the same component.

The various notations are clarified hereafter.

2.2.1.1 Variables of state

the variables are:

- pressures of each components P_p^c
- the temperature of the medium T.

These various variables are not completely independent. Indeed, if only one component is considered, the thermodynamic equilibrium between its phases imposes a relation between the steam pressure and the pressure of the fluid of this component. Finally, there is only one independent pressure per component, just as there is only one conservation equation of the mass. The number of independent pressures is thus equal to the number of independent components. The choice of these pressures is free (combinations of the pressures of the components) provided that the pressures chosen, associated with the temperature, form a system of independent variables.

We chose - and in order to be homogeneous with the finite elements formulation - as variable independent and descriptive of the medium:

- stagnation pressure of gas $P_g=P_g^w+P_g^h$, (model of Dalton)
- fluid stagnation pressure $P_l=P_l^w+P_l^h$
- capillary pressure $P_c=P_g-P_l=P_g^w+P_g^h-(P_l^w+P_l^h)$.

2.2.1.2 Quantities characteristic of the solid phase

One notes:

Porosity: ϕ ,

The intrinsic tensor of permeability: $\mathbf{k}$

2.2.1.3 Quantities characteristic of the fluids

One notes:

- Density of the phase p : ρ_p , $\rho_p=\rho_p^w+\rho_p^h$
- The viscosity of the phase p : μ_p
- The saturation of the phase p : , $S_l+S_g=1$ which is a decreasing function of the capillary pressure. One thus has $S_l=f\left(P_c\right)$.
- The relative permeability of the phase p : k_{rp} function of saturation

- the hydraulic conductivity of the phase p : λ_p^H such as: $\lambda_p^H=\frac{\boldsymbol{k}\, k_{rp}}{\mu_p}$
- The mobility of the component $c, c=(h, w)$ associated with the phase p $k_p^c=\frac{\rho_p^c k_{rp}}{\mu_p}$
- molar mass with the component c : M^c
- Molar concentration $c_p^c=\frac{\rho_p^c}{M^c}$
- mass fraction of the phase p and the component c : $\zeta_p^c=\frac{\rho_p^c}{\rho_p}$
- Molar fraction: $X_p^c=\frac{c_p^c}{c_p}$ where $c_p=c_p^h+c_p^w$ (in the literature, these concentrations are sometimes also noted C_p^c)
- the modulus of compressibility of water K_w

2.3 Constitutive equations of the model

One will not give the details here making it possible to arrive at the final equations of the model. For the intermediate stages, one will refer to [R7.01.11]. One is thus satisfied here with a brief recall of the principal equations.

2.3.1 Balance equations

the balance equations are given here by the conservation of the mass of each component, that is to say:

$$\begin{cases} \dot{m}_l^w+\dot{m}_g^w+Div\left(\boldsymbol{F}_l^w+\boldsymbol{F}_g^w\right)=0 \\ \dot{m}_l^h+\dot{m}_g^h+Div\left(\boldsymbol{F}_l^h+\boldsymbol{F}_g^h\right)=0 \end{cases}$$

with m_p^c the mass contribution of the component c in phase p , such as $m_p^c=\phi . S_p . \rho_p^c$ and $\boldsymbol{F}_p^c$ mass flux of the phase p for the component c .

F_p^c is made up by the mass flux Fickien $\boldsymbol{J}_p^c$ and mass flux Darcéen $\boldsymbol{F}_p$ such as:

$$\boldsymbol{F}_p^c=\boldsymbol{J}_p^c+\rho_p^c\frac{\boldsymbol{F}_p}{\rho_l}, c=(h, w) ; p=(l, g)$$

2.3.2 Equations of behavior

2.3.2.1 Constitutive laws of the fluids

Evolution of porosity:

In the absence of mechanics, one allows nevertheless an evolution of porosity via the coefficient of storage E_m , such as:

$$d\phi=E_m d P_l$$

Behavior fluid:

It is considered that water can be compressible: $\frac{d\rho_l^w}{\rho_l^w}=\frac{dP_l^w}{K_w}$

Behavior gas:

It is considered that the gas is subjected to the model of perfect gases:
$\frac{P_g^c}{\rho_g^c}=\frac{RT}{M^c};c=(w,h)$ where R is the constant of perfect gases.

Model of equilibrium water vapor:

the equilibrium water vapor is written by equality of the free enthali, which, for an isothermal problem gives (confer R7.01.11) :

$$\frac{dP_g^w}{\rho_g^w}=\frac{dP_l^w}{\rho_l^w}$$

Model of equilibrium dry gas /dissous:

The model of Henry connects the component c in his gas form to its liquid form such as:
$P_g^h=K_h\frac{\rho_l^h}{M^h}$ where K_h coefficient of Henry.

Note: one often finds this coefficient in the literature in the form $H=\frac{1}{K_h}$

2.3.2.2 Equations of diffusion

Model of Darcy:

The model of Darcy connects flux $\boldsymbol{F}_p$ of the phase p to its gradient of pressure, such as:

$$\frac{\boldsymbol{F}_p}{\rho_p}=\frac{-\boldsymbol{k}\,k_{rp}}{\mu_p}\left(\nabla P_p-\rho_p\boldsymbol{g}\right)$$
with $\boldsymbol{g}$ gravity

Model of Fick:

One writes the mass flux Fickiens such as:
$\boldsymbol{J}_p^c=-\phi M^c S_p D_p c_p \nabla X_p^c$ where D_p is the coefficient of diffusion (where coefficient of Fick) of the phase p .

One neglects the Fickien flux of water in the fluid (concentration of water in the fluid comparable to 1). With final, one thus obtains:

$$\begin{aligned}
\boldsymbol{F}_l^w&=-\rho_l^w\lambda_l^H\left(\nabla P_l-\rho_l\boldsymbol{g}\right)\\
\boldsymbol{F}_l^h&=-\rho_l^h\lambda_l^H\left(\nabla P_l-\rho_l\boldsymbol{g}\right)-\phi M^h S_l c_l D_l\nabla X_l^h\\
\boldsymbol{F}_g^w&=-\rho_g^w\lambda_g^H\left(\nabla P_g-\rho_g\boldsymbol{g}\right)-\phi M^w S_g c_g D_g\nabla X_g^w\\
\boldsymbol{F}_g^h&=-\rho_g^h\lambda_g^H\left(\nabla P_g-\rho_g\boldsymbol{g}\right)-\phi M^h S_g c_g D_g\nabla X_g^h
\end{aligned}$$

3 The diagrams finished volumes implemented in *Code_Aster*

We present in this chapter the diagrams finished volumes which were implemented in Code_Aster.

3.1 General information on finished volumes

the method of finished volumes consists in integrating one or more equations on a control volume then to discretize flux on each edge of these volumes. Contrary to the finite elements, there is not properly spoke about variational formula.
Let us take the example of an equation of the form $div(\Theta(X,u,\nabla u))=f(x)$. Its approximation on a group $\Omega\subset\mathbb{R}^n$ is a constant function per pieces on a cutting of Ω in control volumes noted thereafter K.
The principle of the method of finished volumes is to integrate the equation on each one of these control volumes. By means of the formula of Green, the equations are written:

$$\int_{\partial K}\Theta(X,u,\nabla u).n_K d\gamma=\int_K f(x)dx,\forall K$$

with n_K the outgoing unit norm of control volume K.

It is seen whereas to apply a diagram finished volumes consists in approaching flux on edges.
For a transitory equation of the type:
$\frac{\partial u}{\partial t}+div(\Theta(X,u,\nabla u))=f(x)$, there will be logically a formulation of the type
$\int_K u\,dx+\int_{\partial K}\Theta(X,u,\nabla u).n_K d\gamma=\int_K f(x)dx,\forall K$

In short, a diagram finished volumes is defined by:

- The choice of the control volume K which can be identical to the mesh, or a construction (of Voronoï type for example). The approximate solution given by the diagrams of finished the volumes type will be constant per pieces on this cutting.
- The position of the nodes of approximation of the unknowns for each volume.
- Way approach flux on an edge of control volume: They are approached by the integral formulation of the equations and the application of the formula of Green on edge of control volume. During the approximation, the flux must be conservative and consistent. The conservativity results in the continuity of flux to the interface, by definition ensured by finished volumes (the flux is written explicitly). Consistency is reached when the difference between real flux and its approximation tends towards 0. There exists one very a large number of diagrams according to the way of calculating this flux and necessary consistency.

The writing of flux can thus connect nodes which do not belong forcing to the same element. They can be connected for example by a common interface. One thus sees that in this case, two nodes are connected, either when they belong to the same element as in finite elements, but when they belong to two neighbors (connected by a common face).

To implement most these diagrams it is thus necessary to resort to the topological notion of vicinity what constitutes an important difference compared to the finite elements.

3.2 Finished volumes SUSHI applied to miscible diphasic flows

diphasic flows in porous environment are governed by the system of equations (3.2.1) :

$$\begin{cases} \dot{m}_l^w+\dot{m}_g^w+Div\left(\boldsymbol{F}_l^w+\boldsymbol{F}_g^w\right)=0 \\ \dot{m}_l^h+\dot{m}_g^h+Div\left(\boldsymbol{F}_l^h+\boldsymbol{F}_g^h\right)=0 \\ P_l(\boldsymbol{x},t)=\tilde{P}_l \quad sur \quad \partial\Omega_d \\ S_l(\boldsymbol{x},t)=\tilde{S}_l \quad sur \quad \partial\Omega_d \\ [\boldsymbol{F}_l^w+\boldsymbol{F}_g^w].\boldsymbol{n}=\phi^w \quad sur \quad \partial\Omega_n \\ [\boldsymbol{F}_l^h+\boldsymbol{F}_g^h].\boldsymbol{n}=\phi^h \quad sur \quad \partial\Omega_n \end{cases} \tag{3.2.1}$$

It is pointed out in addition that the statement of the mass contributions is:

$$\begin{aligned} m_w &= \rho_w \varphi S_{lq} - \rho_w^0 \varphi^0 S_{lq}^0 \\ m_{ad} &= \rho_{ad} \varphi S_{lq} - \rho_{ad}^0 \varphi^0 S_{lq}^0 \\ m_{as} &= \rho_{as} \varphi\left(1-S_{lq}\right)-\rho_{as}^0 \varphi^0\left(1-S_{lq}^0\right) \\ m_{vp} &= \rho_{vp} \varphi\left(1-S_{lq}\right)-\rho_{vp}^0 \varphi^0\left(1-S_{lq}^0\right) \end{aligned} \tag{3.2.2}$$

the flux are then:

$$\begin{aligned} \boldsymbol{F}_l^w &= -\rho_l^w \lambda_l^H\left(\nabla P_l-\rho_l \boldsymbol{g}\right) \\ \boldsymbol{F}_l^h &= -\rho_l^h \lambda_l^H\left(\nabla P_l-\rho_l \boldsymbol{g}\right)-\phi M^h S_l c_l D_l \nabla X_l^h \\ \boldsymbol{F}_g^w &= -\rho_g^w \lambda_g^H\left(\nabla P_g-\rho_g \boldsymbol{g}\right)-\phi M^w S_g c_g D_g \nabla X_g^w \\ \boldsymbol{F}_g^h &= -\rho_g^h \lambda_g^H\left(\nabla P_g-\rho_g \boldsymbol{g}\right)-\phi M^h S_g c_g D_g \nabla X_g^h \end{aligned} \tag{3.2.3}$$

3.2.1 Choice of the unknowns

the usual choice of unknowns (P_c, P_g) is retained in the mesh like on the edges of this one. This choice is in addition compatible with the unified processing of miscible and immiscible flows in saturated and unsaturated medium (see 21).

3.2.2 Choice of control volume

control volume corresponds here to mesh: an element is equal to a control volume.

3.2.3 Writing of flux

the geometrical notations used thereafter for an element K (here triangular, but the principle is the same one for rectangle or in 3D) are indicated Illustration 1.
One will note thereafter L the close triangle with K separated by the interface σ. It is pointed out that the notation $|K|$ indicates its measurement (or surfaces).

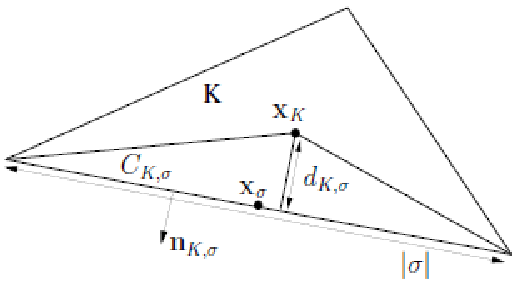

Illustration 1: Representation of the various quantities

We can distinguish various types of flux which we will name thereafter "mass" flux or "voluminal" flux. The mass flux are actually the "physical" flux classics in other words they are the quantities $\int_{\partial K} -\boldsymbol{k} k_p^c \nabla[P_p - \rho_p \boldsymbol{g.x}].\boldsymbol{n_{K,\sigma}} d\gamma$ for the Darcéens terms and $\int_{\partial K} -\phi M^c S_p D_p(S_p) c_p \nabla X_p^c.\boldsymbol{n_{K,\sigma}} d\gamma$ the Fickiens terms.
On the other hand, the voluminal flux are for the Darcéens terms the quantities $\int_{\partial K} -\boldsymbol{k}\nabla[P_p - \rho_p \boldsymbol{g.x}], \boldsymbol{n_{K,\sigma}} d\gamma$ and the Fickiens terms the quantities $\int_{\partial K} -\nabla X_p^c.\boldsymbol{n_{K,\sigma}} d\gamma$. Concretely, one extracts the terms depending on space (via saturation) from computation on voluminal flux.

One of the choices carried out for the extension of the diagram SUSHI to the diphasic nonlinear case is to rather approximate by discrete flux voluminal flux than mass flux. This choice has the advantage of being able to lead to a continuity equation of linear voluminal flux. However, it is then necessary to ensure the continuity of the other discontinuous quantities step of other techniques (for example, by decentring or average). These various approaches are compared in 21.

One then notes the discretization of voluminal flux such as:

- $\int_{\partial K} -\boldsymbol{k}\nabla[P_p - \rho_p \boldsymbol{g.x}], \boldsymbol{n_{K,\sigma}} d\gamma$ by ($\Sigma_{\sigma\in\epsilon_K} F_{p,K,\sigma}(P_p - \rho_p \boldsymbol{g.x}), p\in(l,g)$ one is discretized adds flux for each edge σ pertaining to the group of stop K: ϵ_K).
- $\int_{\partial K} -\nabla X_p^c.\boldsymbol{n_{K,\sigma}} d\gamma$ are discretized par. $\Sigma_{\sigma\in\epsilon_K} \tilde{F}_{p,K,\sigma}(X_p^c), c\in(h,w), p\in(l,g)$

the discretized voluminal flux are thus expressed in the following way:

$$F_{p,K,\sigma}(P_p - \rho_g \boldsymbol{g.x}) = \Sigma_{\sigma'\in\epsilon_K} C_K^{\sigma,\sigma'}[P_{p,K} - P_{p,\sigma'} - \rho_{p,K} \boldsymbol{g.}[\boldsymbol{x_K} - \boldsymbol{x_{\sigma'}}]] \quad (3.2.4)$$

$$\tilde{F}_{p,K,\sigma}(X_p^c) = \sum_{\sigma'\in\epsilon_K} D_K^{\sigma,\sigma'}[X_{p,K}^c - X_{p,\sigma'}^c] \quad (3.2.5)$$

With

$$C_K^{\sigma,\sigma'} = \sum_{\sigma''\in\epsilon_K} \boldsymbol{Y}^{\boldsymbol{\sigma'',\sigma}}.\boldsymbol{k_{K,\sigma''}} \boldsymbol{Y}^{\boldsymbol{\sigma'',\sigma'}} \quad (3.2.6)$$

$$D_K^{\sigma,\sigma'} = \sum_{\sigma''\in\epsilon_K} \boldsymbol{Y}^{\boldsymbol{\sigma'',\sigma}}.\frac{d_{K,\sigma''}|\sigma''|}{d} \boldsymbol{Y}^{\boldsymbol{\sigma'',\sigma'}} \quad (3.2.7)$$

Where:

$$\boldsymbol{k_{K,\sigma''}} = \int_{C_{K,\sigma}} \boldsymbol{k}(\boldsymbol{x}) d\,\boldsymbol{x} = \boldsymbol{k_K} \frac{d_{K,\sigma''}|\sigma''|}{d} \quad (3.2.8)$$

And:

$$Y^{\sigma,\sigma'}=\frac{|\sigma|}{|K|}\boldsymbol{n}_{K,\sigma}+\frac{\beta_K}{d_{k,\sigma}}[1-\frac{|\sigma|}{|K|}\boldsymbol{n}_{K,\sigma}.[\boldsymbol{x}_\sigma-\boldsymbol{x}_K]]\boldsymbol{n}_{k,\sigma}\quad si\quad \sigma=\sigma' \tag{3.2.9}$$

$$Y^{\sigma,\sigma'}=\frac{|\sigma'|}{|K|}\boldsymbol{n}_{K,\sigma'}-\frac{\beta_K}{d_{k,\sigma}|K|}|\sigma'|\boldsymbol{n}_{K,\sigma}.[\boldsymbol{x}_\sigma-\boldsymbol{x}_K]\boldsymbol{n}_{k,\sigma}\quad si\quad \sigma\neq\sigma' \tag{3.2.10}$$

the choice to discretize by the method of Finished Volumes SUSHI only the voluminal flux results in having to treat in a specific way mobilities as well as the terms of Fickiens diffusion. Indeed, the relative permeabilities as well as the tensors of diffusion, present respectively in mobilities and the terms of Fickiens diffusion, are quantities which depend on saturation and which can be heterogeneous.

We will present various possible formulations of the discretization of the equations which govern flows in porous environment, resulting from various decentrings of the nonlinear quantities.

One will note thereafter:

- The equation discretized of conservation of water on the element K : R_K^w
- The equation discretized of conservation of the component gas on the element K : R_K^h
- The equation discretized of continuity of water flux through the interface σ : R_σ^w
- The equation discretized of continuity of flux of the gas component through the interface σ : R_σ^h

3.2.4 Decentring

the phenomenon dominating in diphasic flows in porous environment is the diffusion Darcéenne, we will thus focus itself on the study of the continuity of mobilities $\rho_p\frac{k_{r,p}}{\mu_p}$. The terms of Fickiens diffusion will be looked in the second place so only ensuring their assured continuity once that of mobilities.

When we are in the presence of nonlinear terms which depend on space, here mobilities, we must ensure their continuity in the event of heterogeneous problem. For that we can decentre them. The decentring of mobilities aims to ensure the monotony and the stability of the diagrams. However, it decreases the accuracy of computations by adding numerical diffusion. There exist many decentrings in the literature, the nonlinear term of mobility $\rho_p\frac{k_{r,p}}{\mu_p}$ depending on space, being able to be calculated by various diagrams:

- the diagram upstream which decentres this term according to the meaning of the flow of the phase in the current mesh or the close mesh by the edge considered,
- the causal diagram which will decentre this term differently when it is factor of a term of pressure or factor of a term of gravity. Decentring will be done all the same in the current mesh or the close mesh,
- the diagram with Peclet number variable who allows to break up the convective part of flux into a linear combination between eccentric flux of the diagram upstream and centered flux. Thus the parameter of this combination can be adjusted locally on each edge according to the diffusion introduced by the capillary pressure.

We will present below the three formulations retained in Code_Aster, two of them will decentre by the diagram upstream mobilities, either on the edge of the mesh current or on the close mesh by the edge and the third formulation will use the mobilities centered in the current mesh. We decided to preserve these 3 formulations, but we will have thereafter the advantages or objections of each one.

First formulation: eccentric diagram Finished Volumes Nets (VFDM)

This formulation consists in using a decentring in the mesh close by phase to mobilities in order to treat heterogeneities correctly. In other words, if it is considered that element σ stops it K separates it from the close element L :

$$\begin{array}{llll} Si & F_{p,K,\sigma}\geqslant 0 & alors & k_p^c=k_p^c(P_{p,K}) \\ Si & F_{p,K,\sigma}<0 & alors & k_p^c=k_p^c(P_{p,L}) \end{array} \quad (3.2.11)$$

This kind of decentring is usually used under the name of diagram simple upstream (or diagram of the tankers).
The continuity of mobilities being ensured by decentring, we do not have any more that to impose explicitly the continuity of the voluminal flux Darcéens for the fluid and gas. We thus impose continuity through the interfaces on the quantities $\int_{\partial K} -\boldsymbol{k}\nabla[P_l-\rho_l \boldsymbol{g}.\boldsymbol{x}],\boldsymbol{n}_{\boldsymbol{K},\boldsymbol{\sigma}} d\gamma$ and $\int_{\partial k} -\boldsymbol{k}\nabla[P_g-\rho_g \boldsymbol{g}.\boldsymbol{x}],\boldsymbol{n}_{\boldsymbol{K},\boldsymbol{\sigma}} d\gamma$.

Remain to ensure the continuity of the terms of molecular diffusion. The latter is guaranteed by carrying out an average, between the current mesh and the close mesh by the edge considered, of the mass flux Fickiens in the conservation equations of the mass.

The disadvantage of this discretization comes owing to the fact that we must then distinguish the edges from edges of the internal edges. We thus write for the edge edges the continuity of mass flux of the terms Darcéens and Fickiens. Same way, for the edge edges, we center mobilities and the terms of diffusion in the mesh costing in the conservation equation of the mass.
In the system of equations (3.2.1), we can distinguish two types of edges from edge, those where conditions of Dirichlet are imposed and those where are conditions of Neumann. Nevertheless, only those where conditions of Neumann are applied present a difficulty, we will thus present only the discretization of the system of equations (3.2.1) on the internal edges and this kind of edge edges ∂_n .

In the following notations, the exhibitor "" $._{}^{-}$ corresponds to previous time.

$$
Si\ \ \sigma\in\epsilon_{K,inter}\ \ alors
$$

$$
\left|
\begin{array}{l}
eq.\ R_K^w:\\
\frac{|K|}{\Delta t}[m_{l,K}^w-m_{l,K}^{w,-}]+\frac{|K|}{\Delta t}[m_{g,K}^w-m_{g,K}^{w,-}]\\
+\sum_{\sigma\in\epsilon_{K,inter}}[k_{l,\sigma}^w F_{l,K,\sigma}(P_l-\rho_l\boldsymbol{g.x})+k_{g,\sigma}^w F_{g,K,\sigma}(P_g-\rho_g\boldsymbol{g.x})]\\
+\sum_{\sigma\in\epsilon_{K,inter}}\frac{1}{2}[\phi_K M^w S_{g,K}D_{g,K,\sigma}c_{g,K}\tilde{F}_{g,K,\sigma}(X_g^w)-\phi_L M^w S_{g,L}D_{g,L,\sigma}c_{g,L}\tilde{F}_{g,L,\sigma}(X_p^w)]\\
=0\\
eq.\ R_\sigma^w:\\
F_{l,K,\sigma}(P_l-\rho_l\boldsymbol{g.x})+F_{l,L,\sigma}(P_l-\rho_l\boldsymbol{g.x})=0\\
\\
eq.\ R_K^h:\\
\frac{|K|}{\Delta t}[m_{l,K}^h-m_{l,K}^{h,-}]+\frac{|K|}{\Delta t}[m_{g,K}^h-m_{g,K}^{h,-}]\\
+\sum_{\sigma\in\epsilon_{K,inter}}[k_{l,\sigma}^h F_{l,K,\sigma}(P_l-\rho_l\boldsymbol{g.x})+k_{g,\sigma}^h F_{g,K,\sigma}(P_g-\rho_g\boldsymbol{g.x})]\\
+\sum_{\sigma\in\epsilon_{K,inter}}\sum_{p\in(l,g)}\frac{1}{2}[\phi_K M^h S_{p,K}D_{p,K,\sigma}c_{p,K}\tilde{F}_{p,K,\sigma}(X_p^h)-\phi_L M^h S_{p,L}D_{p,L,\sigma}c_{p,L}\tilde{F}¿p,\\
=0\\
eq.\ R_\sigma^h:\\
F_{g,K,\sigma}(P_g-\rho_g\boldsymbol{g.x})+F_{g,L,\sigma}(P_g-\rho_g\boldsymbol{g.x})=0
\end{array}
\right.
\qquad (3.2.12)
$$

$$
\text{Sinon} \quad si\,\sigma \in \epsilon_{K,ext} \quad alors
$$

$$
\left|
\begin{array}{l}
eq.\ R_K^w: \\
\frac{|K|}{\Delta t}[m_{l,K}^w - m_{l,K}^{w,-}] + \frac{|K|}{\Delta t}[m_{g,K}^w - m_{g,K}^{w,-}] \\
+\sum_{\sigma\in\epsilon_{K,ext}} [k_{l,K}^w F_{l,K,\sigma}(P_l - \rho_l \boldsymbol{g.x}) + k_{g,K}^w F_{g,K,\sigma}(P_g - \rho_g \boldsymbol{g.x})] \\
+\sum_{\sigma\in\epsilon_{K,ext}} \phi_K M^w [S_{g,K} D_{g,K,\sigma} c_{g,K} \tilde{F}_{g,K,\sigma}(X_g^w)] = 0 \\
eq.\ R_\sigma^w: \\
k_{l,K}^w F_{l,K,\sigma}(P_l - \rho_l \boldsymbol{g.x}) + k_{g,K}^w F_{g,K,\sigma}(P_g - \rho_g \boldsymbol{g.x}) \\
+\phi_K M^w S_{g,K} D_{g,K,\sigma} c_{g,K} \tilde{F}_{g,K,\sigma}(X_g^w) = \phi^w \\
\\
eq.\ R_K^h: \\
\frac{|K|}{\Delta t}[m_{l,K}^h - m_{l,K}^{h,-}] + \frac{|K|}{\Delta t}[m_{g,K}^h - m_{g,K}^{h,-}] + \sum_{\sigma\in\epsilon_{K,inter}} [k_{l,K}^h F_{l,K,\sigma}(P_l - \rho_l \boldsymbol{g.x})] \\
+\sum_{\sigma\in\epsilon_{K,ext}} [k_{g,K}^h F_{g,K,\sigma}(P_g - \rho_g \boldsymbol{g.x})] + \sum_{p\in(l,g)} \phi_K M^h S_{p,K} D_{p,K,\sigma} c_{p,K} \tilde{F}_{p,K,\sigma}(X_p^h) \\
=0 \\
eq.\ R_\sigma^h: \\
k_{l,K}^h F_{l,K,\sigma}(P_l - \rho_l \boldsymbol{g.x}) + k_{g,K}^h F_{g,K,\sigma}(P_g - \rho_g \boldsymbol{g.x}) \\
+\phi_K M^h S_{g,K} D_{g,K,\sigma} c_{g,K} \tilde{F}_{g,K,\sigma}(X_g^w) + \phi_K M^h S_{l,K} D_{l,K,\sigma} c_{l,K} \tilde{F}_{l,K,\sigma}(X_l^w) = \phi^h
\end{array}
\right.
\qquad (3.2.13)
$$

With ϕ^c which represents physical flux resulting from the boundary conditions of Neumann.

However, this formulation quickly reveals a major drawback: the decentring of mobilities as of the terms of diffusion oblige of the mesh to know all the neighbors by edges current and thus with calculating and storing data concerning all the neighbors. We will then have a jacobian matrix, resulting from the resolution of the nonlinear, full problem and the time of resolution of diphasic flows with this formulation will be thus important.

Second formulation: diagram Finished Volumes Centered (VFC)

the purpose of this formulation is to reduce the profile of the jacobian matrix which will intervene during the resolution of the nonlinear problem. Indeed, the preceding formulation had the disadvantage of using the meshes close ones by edge of the mesh current. In this formulation, we wished to free ourselves from this disadvantage. For that, we decide not to more carry out decentring of mobilities nor of average of the terms of diffusion in the conservation equation of the mass and we will write simply the continuity of the mass flux Darcéens and Fickiens.
We thus write continuity on the following quantities:

$$
\int_{\partial K} \left[-\boldsymbol{k}\, k_l^w \nabla [P_l - \rho_l \boldsymbol{g.x}] - \boldsymbol{k}\, k_g^w \nabla [P_g - \rho_g \boldsymbol{g.x}] - \phi M^w S_g D_g c_g \nabla X_g^w \right] . \boldsymbol{n}_{K,\sigma} d\gamma \quad \text{and}
$$

$$
\int_{\partial K} \left[-\boldsymbol{k}\, k_l^h \nabla [P_l - \rho_l \boldsymbol{g.x}] - \boldsymbol{k}\, k_g^h \nabla [P_g - \rho_g \boldsymbol{g.x}] - \phi M^h S_g D_g c_g \nabla X_g^h - \phi M^h S_l D_l c_l \nabla X_l^h \right] . \boldsymbol{n}_{K,\sigma} d\gamma
$$

Moreover, this writing makes it possible to be freed from the need for differentiating the edges from edge from the internal edges.

The discretization of the first two equations of the system (3.2.1) is written in the following way:

$$\left|\begin{array}{l}
eq.\,R_K^w:\\
\frac{|K|}{\Delta t}[m_{l,K}^w-m_{l,K}^{w,-}]+\frac{|K|}{\Delta t}[m_{g,K}^w-m_{g,K}^{w,-}]+\sum_{\sigma\in\epsilon_{K,ext}}[k_{l,K}^w F_{l,K,\sigma}(P_l-\rho_l\,\boldsymbol{g.x})]\\
+\sum_{\sigma\in\epsilon_{K,ext}}[k_{g,K}^w F_{g,K,\sigma}(P_g-\rho_g\,\boldsymbol{g.x})+\phi_K M^w S_{g,K} D_{g,K,\sigma} c_{g,K} \tilde{F}_{g,K,\sigma}(X_g^w)]=0\\
eq.\,R_\sigma^w:\\
k_{l,K}^w F_{l,K,\sigma}(P_l-\rho_l\,\boldsymbol{g.x})+k_{g,K}^w F_{g,K,\sigma}(P_g-\rho_g\,\boldsymbol{g.x})\\
+\phi_K M^w S_{g,K} D_{g,K,\sigma} c_{g,K} \tilde{F}_{g,K,\sigma}(X_g^w)+k_{l,L}^w F_{l,L,\sigma}(P_l-\rho_l\,\boldsymbol{g.x})\\
+k_{g,L}^w F_{g,L,\sigma}(P_g-\rho_g\,\boldsymbol{g.x})+\phi_L M^w S_{g,L} D_{g,L,\sigma} c_{g,L} \tilde{F}_{g,L,\sigma}(X_g^w)=0\\
\\
eq.\,R_K^h:\\
\frac{|K|}{\Delta t}[m_{l,K}^h-m_{l,K}^{h,-}]+\frac{|K|}{\Delta t}[m_{g,K}^h-m_{g,K}^{h,-}]+\sum_{\sigma\in\epsilon_{K,inter}}[k_{l,K}^h F_{l,K,\sigma}(P_l-\rho_l\,\boldsymbol{g.x})]\\
+\sum_{\sigma\in\epsilon_{K,inter}}[k_{g,K}^h F_{g,K,\sigma}(P_g-\rho_g\,\boldsymbol{g.x})]+\sum_{p\in(l,g)}\phi_K M^h S_{p,K} D_{p,K,\sigma} c_{p,K} \tilde{F}_{p,K,\sigma}(X_p^h)\\
=0\\
eq.\,R_\sigma^h:\\
k_{l,K}^h F_{l,K,\sigma}(P_l-\rho_l\,\boldsymbol{g.x})+k_{g,K}^h F_{g,K,\sigma}(P_g-\rho_g\,\boldsymbol{g.x})\\
+\phi_K M^h S_{g,K} D_{g,K,\sigma} c_{g,K} \tilde{F}_{g,K,\sigma}(X_g^w)+\phi_K M^h S_{l,K} D_{l,K,\sigma} c_{l,K} \tilde{F}_{l,K,\sigma}(X_l^w)\\
k_{l,L}^h F_{l,L,\sigma}(P_l-\rho_l\,\boldsymbol{g.x})+k_{g,L}^h F_{g,L,\sigma}(P_g-\rho_g\,\boldsymbol{g.x})\\
+\phi_L M^h S_{g,L} D_{g,L,\sigma} c_{g,L} \tilde{F}_{g,L,\sigma}(X_g^w)+\phi_L M^h S_{l,L} D_{l,L,\sigma} c_{l,L} \tilde{F}_{l,L,\sigma}(X_l^w)=0
\end{array}\right. \quad (3.2.14)$$

the default of this formulation comes from the absence of decentring, which can pose heterogeneous problems of problems during the resolution, for example during a case representing the juxtaposition of two very contrasted materials. Indeed, the fact of centering mobilities decreases the monotony and thus the stability of the diagram. We are thus likely to have oscillations with the interface of the materials.
However, if the problem to be solved does not have heterogeneity of the physical properties, then this formulation will make it possible to give good performances while having a reasonable profile.

Third formulation: eccentric diagram Finished Volumes Edge (VFDA)

the interest of this formulation is at the same time to keep the notion of decentring, while keeping a small stencil of the jacobian matrix. For that, we continue to write the continuity of mass total flux but we of the mesh decentre mobilities on the edges current. We thus consider the continuity of the following quantities:

$$\int_{\partial K}\left[-\boldsymbol{k}\,k_l^w\nabla[P_l-\rho_l\,\boldsymbol{g.x}]-\boldsymbol{k}\,k_g^w\nabla[P_g-\rho_g\,\boldsymbol{g.x}]-\phi M^w S_g D_g c_g\nabla X_g^w\right].\boldsymbol{n}_{K,\sigma}\,d\gamma$$

and

$$\int_{\partial K}\left[-\boldsymbol{k}\,k_l^h\nabla[P_l-\rho_l\,\boldsymbol{g.x}]-\boldsymbol{k}\,k_g^h\nabla[P_g-\rho_g\,\boldsymbol{g.x}]-\phi M^h S_g D_g c_g\nabla X_g^h-\phi M^h S_l D_l c_l\nabla X_l^h\right].\boldsymbol{n}_{K,\sigma}\,d\gamma$$

decentring is written then:

$$\begin{array}{l} Si \quad F_{p,K,\sigma} \geq 0 \quad alors \quad k^c_{p,K,\sigma} = k^c_p(P_{p,K}) \\ Si \quad F_{p,K,\sigma} < 0 \quad alors \quad k^c_{p,K,\sigma} = k^c_p(P_{p,\sigma}) \end{array} \quad (3.2.15)$$

With regard to the terms of Fickiens diffusion, since the molecular diffusion is not the phenomenon dominating, we decide not to apply particular processing to them and we will thus take their values in the current mesh.

Thus we will be able, as in the second formulation, and the not to make the distinction between the internal edges edge edges. A flat with this formulation could be that final we ensure doubly the continuity of the mass flux Darcéens since they are continuous thanks to the equations of continuity of flux but also thanks to their writing in the conservation of the mass.

In spite of that this formulation seems to be able to be powerful. Indeed, it does not use the neighbors of the edges, which enables him to have a weak time of resolution. In addition, it makes it possible to solve heterogeneous problems.

The discretization of the first two equations of the system (3.2.1) is written in the following way:

$$\left| \begin{array}{l} eq.\ R^w_K : \\ \frac{|K|}{\Delta t}[m^w_{l,K} - m^{w,-}_{l,K}] + \frac{|K|}{\Delta t}[m^w_{g,K} - m^{w,-}_{g,K}] + \sum_{\sigma \in \epsilon_{K,ext}} [k^w_{l,K,\sigma} F_{l,K,\sigma}(P_l - \rho_l \boldsymbol{g.x})] \\ + \sum_{\sigma \in \epsilon_{K,ext}} [k^w_{g,K,\sigma} F_{g,K,\sigma}(P_g - \rho_g \boldsymbol{g.x}) + \phi_K M^w S_{g,K} D_{g,K,\sigma} c_{g,K} \tilde{F}_{g,K,\sigma}(X^w_g)] = 0 \\ eq.\ R^w_\sigma : \\ k^w_{l,K,\sigma} F_{l,K,\sigma}(P_l - \rho_l \boldsymbol{g.x}) + k^w_{g,K,\sigma} F_{g,K,\sigma}(P_g - \rho_g \boldsymbol{g.x}) \\ + \phi_K M^w S_{g,K} D_{g,K,\sigma} c_{g,K} \tilde{F}_{g,K,\sigma}(X^w_g) + k^w_{l,L,\sigma} F_{l,L,\sigma}(P_l - \rho_l \boldsymbol{g.x}) \\ + k^w_{g,L,\sigma} F_{g,L,\sigma}(P_g - \rho_g \boldsymbol{g.x}) + \phi_L M^w S_{g,L} D_{g,L,\sigma} c_{g,L} \tilde{F}_{g,L,\sigma}(X^w_g) = 0 \\ \\ eq.\ R^h_K : \\ \frac{|K|}{\Delta t}[m^h_{l,K} - m^{h,-}_{l,K}] + \frac{|K|}{\Delta t}[m^h_{g,K} - m^{h,-}_{g,K}] + \sum_{\sigma \in \epsilon_{K,inter}} [k^h_{l,K,\sigma} F_{l,K,\sigma}(P_l - \rho_l \boldsymbol{g.x})] \\ + \sum_{\sigma \in \epsilon_{K,inter}} [k^h_{g,K,\sigma} F_{g,K,\sigma}(P_g - \rho_g \boldsymbol{g.x})] + \sum_{p \in (l,g)} \phi_K M^h S_{p,K} D_{p,K,\sigma} c_{p,K} \tilde{F}_{p,K,\sigma}(X^h_p) \\ = 0 \\ eq.\ R^h_\sigma : \\ k^h_{l,K,\sigma} F_{l,K,\sigma}(P_l - \rho_l \boldsymbol{g.x}) + k^h_{g,K,\sigma} F_{g,K,\sigma}(P_g - \rho_g \boldsymbol{g.x}) \\ + \phi_K M^h S_{g,K} D_{g,K,\sigma} c_{g,K} \tilde{F}_{g,K,\sigma}(X^w_g) + \phi_K M^h S_{l,K} D_{l,K,\sigma} c_{l,K} \tilde{F}_{l,K,\sigma}(X^w_l) \\ k^h_{l,L,\sigma} F_{l,L,\sigma}(P_l - \rho_l \boldsymbol{g.x}) + k^h_{g,L,\sigma} F_{g,L,\sigma}(P_g - \rho_g \boldsymbol{g.x}) \\ + \phi_L M^h S_{g,L} D_{g,L,\sigma} c_{g,L} \tilde{F}_{g,L,\sigma}(X^w_g) + \phi_L M^h S_{l,L} D_{l,L,\sigma} c_{l,L} \tilde{F}_{l,L,\sigma}(X^w_l) = 0 \end{array} \right. \quad (3.2.16)$$

4 Put in work in Code_Aster

In this chapter, we specify how are integrated the relations described into chapter 3.

Attention **finished volumes are currently available only with coupling law the hydraulic HYDR_VGM which makes it possible to correctly manage the appearance/disparation of phase by treating negative capillary pressures. Only the model hydraulics now available is thus of the type Mualem Van-Genuchten.**

4.1 Description of the elements

6 types of modelizations exist according to the diagram used:

Modelization	Diagram corresponding	compatible flow Model
D_PLAN_HH2SUC	VFDC	LIQU_AD_GAZ_VAPE, LIQU_AD_GAZ
D_PLAN_HH2SUDA	VFDA	LIQU_AD_GAZ_VAPE, LIQU_AD_GAZ
D_PLAN_HH2SUDM	VFDM	LIQU_AD_GAZ_VAPE, LIQU_AD_GAZ
3D_HH2SUC	VFDC	LIQU_AD_GAZ_VAPE, LIQU_AD_GAZ
3D_HH2SUDA	VFDA	LIQU_AD_GAZ_VAPE, LIQU_AD_GAZ
3D_HH2SUDM	VFDM	LIQU_AD_GAZ_VAPE, LIQU_AD_GAZ

Table 4.1-1: Model finished volumes

the principal unknowns are the capillary pressure (PRE1) and the gas pressure (PRE2) and are located at the center of meshes like in the mediums of the edges (cf Illustration 2.

Illustration 2: Quadratic element

What thus gives for a quadrangle a storage of the kind:

Support	DDL
Face $\sigma 1$	PRE1
	PRE2
Face $\sigma 2$	PRE1
	PRE2
Face $\sigma 3$	PRE1
	PRE2
Face $\sigma 4$	PRE1
	PRE2
Centers K	PRE1
	PRE2

Table 4.1-2: Storage of the unknowns

the elements meshes are defined in 2D for triangles with 7 nodes and quadrilaterals with 9 nodes (“unutilised” tops + mediums of stop + center) like in 3D for hexahedrons with 27 nodes.
One does not have elements of meshes which would exclude the nodes tops but the latter are not taken into account (cf Illustration 2.

4.2 Computation of the stresses and generalized strains

the diagrams finished volumes profit largely from definite structure for the finite elements in [R7.01.10] and [R7.01.11].

Thus the generalized stresses in the center of the element are physically the same ones as in finite elements, namely:
$m_l^w, \mathbf{F_l^w}; m_g^w, \mathbf{F_g^w}; m_g^h, \mathbf{F_g^h}; m_l^h, \mathbf{F_l^h}$ as well as the generalized strains: $p_c, \nabla p_c; p_g, \nabla p_g$.

With the interfaces on the other hand, the flux contain in fact the necessary one to the continuity equation. This last can be different according to the diagram used (see section 10).

For diagram VFDM, the continuity of flux is treated differently according to whether one is with edge or not. Thus, table 4.2-1 lists the various cases for an element K and its interfaces:

Name of component Aster	Contained in the center of K	Contents on the sides $\sigma \epsilon \delta K$	
		Face Interns	edge Face M11
	$\rho_l^w \varphi S_l - (\rho_l^w \varphi S_l)^-$	0	
FH11*	$\sum_{\delta K} \boldsymbol{F_l^w} . \boldsymbol{n}$	$F_{l,K,\sigma}$	$\boldsymbol{F_l^w} . \boldsymbol{n_{K,\sigma}} + \boldsymbol{F_g^w} . \boldsymbol{n_{K,\sigma}}$
M12	$\rho_g^w \varphi S_g - (\rho_g^w \varphi S_g)^-$	0	
FH12*	$\sum_{\delta K} \boldsymbol{F_g^w} . \boldsymbol{n}$	$F_{g,K,\sigma}$	$\boldsymbol{F_l^h} . \boldsymbol{n_{K,\sigma}} + \boldsymbol{F_g^h} . \boldsymbol{n_{K,\sigma}}$
M21	$\rho_g^h \varphi S_l - (\rho_g^h \varphi S_g)^-$	0	
FH21*	$\sum_{\delta K} \boldsymbol{F_g^h} . \boldsymbol{n}$	0	
M22	$\rho_l^h \varphi S_l - (\rho_l^h \varphi S_l)^-$	0	
FH22*	$\sum_{\delta K} \boldsymbol{F_l^h} . \boldsymbol{n}$	0	

Table 4.2-1: Generalized stresses for diagram VFDM (*HH2SUDM)

For diagrams VFDA and VFC, there is no more distinction:

Name of component Aster	Contained in the center of K	Contents on the sides $\sigma\epsilon\delta K$
M11	$\rho_l^w \varphi S_l-(\rho_l^w \varphi S_l)^-$	0
FH11*	$\sum_{\delta K} \boldsymbol{F}_l^w.\boldsymbol{n}$	$\boldsymbol{F}_l^w.\boldsymbol{n}_{K,\sigma}+\boldsymbol{F}_g^w.\boldsymbol{n}_{K,\sigma}$
M12	$\rho_g^w \varphi S_g-(\rho_g^w \varphi S_g)^-$	0
FH12*	$\sum_{\delta K} \boldsymbol{F}_g^w.\boldsymbol{n}$	$\boldsymbol{F}_l^h.\boldsymbol{n}_{K,\sigma}+\boldsymbol{F}_g^h.\boldsymbol{n}_{K,\sigma}$
M21	$\rho_g^h \varphi S_l-(\rho_g^h \varphi S_g)^-$	0
FH21*	$\sum_{\delta K} \boldsymbol{F}_g^h.\boldsymbol{n}$	0
M22	$\rho_l^h \varphi S_l-(\rho_l^h \varphi S_l)^-$	0
FH22*	$\sum_{\delta K} \boldsymbol{F}_l^h.\boldsymbol{n}$	0

Table 4.2-2: Generalized stresses for diagrams VFDA (*HH2SUDA) and VFC (*HH2SUC)

4.3 Integration

As in finite elements, the principal loop of integration is done by element. On the other hand within an element one will buckle on the nodes (there is no more notion of points of integration, but just of the points of approximation which are the nodes here). This diagram having its nodes in the center like on each edge, that makes it possible here implicitly to make a loop on the interfaces. Finally, the structure finite elements is not modified.

With final one can summarize the integration of the various equations treated in the following table (written for a quadrangle but easily generalizable):

Standard	support	Equation
Face $\sigma 1$	$R_{\sigma 1}^w$	Continuity flux of water
	$R_{\sigma 1}^h$	Continuity flux of h
Face $\sigma 2$	$R_{\sigma 2}^w$	Continuity flux of water
	$R_{\sigma 2}^h$	Continuity flux of h
Face $\sigma 3$	$R_{\sigma 3}^w$	Continuity flux of water
	$R_{\sigma 3}^h$	Continuity flux of h
Face $\sigma 4$	$R_{\sigma 4}^w$	Continuity flux of water
	$R_{\sigma 4}^h$	Continuity flux of h
Center K	R_K^w	Conservation of the mass of water

	R_K^h	Conservation of the mass of h

4.4 Local variables

the local variables are here:

Number	Name of component Aster	Contained
1	$V1$	$\rho_{lq} - \rho_{lq}^0$
2	$V2$	$\varphi - \varphi^0$
3	$V3$	$p_{vp} - p_{vp}^0$
4	$V4$	S_{lq}
5	$V5$	P_c
6	$V6$	P_g

Note: : it is pointed out that here Gauss points with the meaning Aster are the nodes of the element.

4.5 Validation

the following table presents some examples of case tests of validation for classical physical problems:

Case test	Phenomenon	Modelizations tested
wtnp117	capillary Rebalancing	D_PLAN_HH2SUDM (c) D_PLAN_HH2SUDA (d)
wtnp120	Appearance/disappearance of phase in a bar	D_PLAN_HH2SUDM (A) D_PLAN_HH2SUDA (b) D_PLAN_HH2SUC (c) 3D_HH2SUDM (E) 3D_HH2SUDA (F) 3D_HH2SUC (G)
wtnp121	Bar saturated with water subjected to a shock with pressure	D_PLAN_HH2SUDM (A) D_PLAN_HH2SUDA (b) D_PLAN_HH2SUC (c) 3D_HH2SUDM (I) 3D_HH2SUDA (J) 3D_HH2SUC (K)
wtnp122	Bar saturated with gas subjected to a shock with pressure	D_PLAN_HH2SUDM (A) D_PLAN_HH2SUDA (b) D_PLAN_HH2SUC (c)
gas	goshawks wtnp123 Injection with a gallery	D_PLAN_HH2SUDM (A) D_PLAN_HH2SUDA (b) D_PLAN_HH2SUC (c)
wtnp124	Test with Liakopoulos: gravitating drainage of a water column	D_PLAN_HH2SUDM (A) D_PLAN_HH2SUDA (b)

5 Bibliography

[1] O. Angelini: “Study of the numerical diagrams for diphasic flows in deformable porous environments for unspecified meshes. Application to the storage of the radioactive waste. Thesis of Ophélie Angélini. ” Note H-T64-2011-01146

[2] S. Granet: “Numerical Building site in THM in Code_Aster” Notes HT-64-2005-01621

[3] Eymard R., Gallouët, T., Herbin R. (2000) “Finite Volume Method”, Handbook of Numerical Analysis, vol. VII, p. 713-1020. Editors: P.G. Ciarlet and J.L. Lions.

[4] Eymard R., Gallouët, T., Herbin R. (2007) “A New Finite Volume general Design fpr anisotropic diffusion problems one grids: convergence analysis”, C.R., Maths, Acoad. Sci. Paris, flight 344, No 6, pp.403-406.

[5] O. Coussy: “Mechanics of porous media”. EDITIONS TECHNIP.

6 Description of the versions of the document

Version Aster	**Author (S) Organization (S)**	**Description of the modifications**
02/10/10	S.Granet EDF-R&D/AMA	initial Version